Signal Processing and Renewable Energy
June 2021, (pp. 15-34)
ISSN: 2588-7327
eISSN: 2588-7335

Investigating the Effect of Different Penetration of Renewable Energy Resources on Islanded Microgrid Frequency Control Using a Robust Method

Amir Hosein Tayebi [1], Reza Sharifi *[2], Amir Hosein Salemi [1], and Faramarz Faghihi [3]

[1] Department of Electrical Engineering, Arak Branch, Islamic Azad University, Arak, Iran.
[2] Department of Electrical Engineering, West Tehran Branch, Islamic Azad University, Tehran, Iran.
[3] Department of Electrical Engineering, Science and Research Branch, Islamic Azad University, Tehran, Iran

Received: 11-Dec-2020, Revised: 26-Dec-2020, Accepted: 29-Dec-2020.

Abstract

This paper proposes a robust method for frequency control in an islanded microgrid facing solar unit uncertainties. Here, microgrids with photovoltaic panels, battery energy storage systems, diesel generators, and fuel cells are considered. This paper focuses on the frequency constancy of stand-alone microgrids for reaction to these uncertainties. There are so many ways to control the frequency of microgrids, such as the PI control method, but these methods can't be useful in the case of uncertain systems. Due to the small scale of energy generation, the microgrid inertia changes with these uncertainties. Robust control is a method for frequency control that can be used in a situation of uncertainties, perturbations and frequency instability. In this article H_∞ frequency control is used for a microgrid with a dual peak load profile in the case of different coefficient penetrations of the solar panel. The results demonstrated that the battery energy storage system's coefficient penetration and the solar cell significantly affect microgrid frequency. A smart algorithm is proposed to determine the best coefficient penetration value for battery energy storage system available electricity and solar panels.

Keywords: Battery energy storage system, Islanded microgrid, Robust frequency control, Solar cell penetration, Uncertainty parameters.

1. INTRODUCTION

The use of distributed generation resources has flourished in recent decades so that due to the tremendous benefits of this type of energy generation, there is a global focus on the use of these resources. One of the issues

*Corresponding Authors Email: Sharifi.r@wtiau.ac.ir

in using of these distributed energy resources, according to their problems, is to provide a suitable platform for the optimal use of these resources. Due to these resources' random generation profile, using them is a very important subject [1]. Microgrids are an economically and functionally optimal platform for exploiting distributed generation resources. In addition to good energy efficiency, this structure provides greater reliability and economic and environmental benefits [2]. Microgrids are low voltage distribution systems with distributed energy sources. Microgrids can be coupled to the main grid or islanded from the main grid based on the working situations, the microgrid's status, and the main power grid [3]. Because the structure of distributed generation resources and their position in the network is flexible, microgrids require an intelligent control system. However, variations in distributed generation resource production pose serious challenges, especially in microgrids' islanding mode [4]. Without support from the leading network, the control of an independent operation MG is often more intricate than the grid-connected one. The direct connection of various renewable energy sources, such as WT, PV, BESS, MT, and FC, to the utility grid, may cause problems of frequency control [5]. During the islanded operation, in the absence of an effective power balance strategy, the frequency may get into high fluctuations and inconsistencies due to the high permeation of renewable resources. In these situations, micro-grids' control is essential to enhance the micro-grid act in real-time, mainly under a high penetration level of DG resources [6]. A widely used control technique for the distributed energy resources inverters is the droop control, which was initially proposed in [7] to coordinate synchronous generators. The droop control permits properly supporting the power demands without communication among the inverters.

In recent years, attention to the multi-agent system technique has been growing to deal with the complexity and distributed problems in electrical power engineering [8]. The multi-agent system technology is being investigated in various power engineering applications, including system restoration, disturbance diagnosis, and secondary voltage control.

The microgrid's primary droop control preserves the voltage and frequency permanency while balancing the generation and load with appropriate power-sharing. The secondary controller recompenses the voltage and frequency deviations from their reference values [9]. To dominate the detriments of the existing microgrid control approaches, various challenges associated with robustness to load uncertainties, the design of decentralized controllers with minimum communication links between DGs, and the low-complexity of the local controllers must be addressed [10].

Due to the small size and consequently small inertia of microgrids, changes in the production values of distributed generation resources or loads can cause changes in system model parameters. As a result, robust control methods are used that are resistant to these changes. In [11] and [12], robust frequency control methods for microgrids have been investigated. The fundamental theory of the H_∞ control is finding a

controller which is based on data in measured outputs and generates control signals which neutralize the impact of disturbances on controlled outputs. The H_∞ control method is applied to be robust and steady against load disturbances, a random outage of slave units, error in the operation of circuit breakers, measurement transmission data error and MG parameters uncertainties [13], [14].

In [15] and [16], a robust controller designed for a power system and its performance is examined. However, due to the importance of microgrids and their operation's upward trend, the use of this control method for microgrids has been considered [17], [18]. In [19] and [20], the effect of the type of resources and loads (including the use of dynamic loads and electric vehicles) in a power system has been investigated. Also, in [21] and [22], frequency control methods in networks with variable inertia have been investigated. The H_∞ control method of robust control methods has been studied in [23] and [24]. One of the factors that can affect microgrids' frequency is the discussion of cybersecurity and the destruction of cyber-physical systems [25].
In [26] and [27], studies have been conducted on the performance of power system converters used in power systems' structure. In [28] and [29] (unlike this paper, which studies the control method for a microgrid), examine the frequency control of multistage power networks. Robust control methods have many applications in controlling various systems. In [30] and [31], this type of controller's performance in different structures has been investigated. One of the important issues that should be considered in microgrids discussion is the controller's steady-state performance [32], [33].

The weighting functions used in the controllers' structure play an important role in their proper performance [34], [35]. Different microgrid structures, including provisional microgrids, are among the topics that have been considered [36], [37]. In [38], an algorithm is proposed to select the appropriate weighting functions in a provisional microgrid.

A DG system based on a PV array generation is considered in this paper. Finding such a structure is because solar energy is a widespread and environment-friendly energy resource readily available in most areas. The periodic feature of the power generated and the random character are two imperfections of the solar irradiance that have adverse effects on the microgrid system's performance. Also, a fuel cell energy generator and a diesel generator are used to generate power and compensate for photovoltaic generation's absence at night. BESS is also used to save additional power and release DG power when production is decreased [39], [40].

A H_∞ controller is also used to control the power produced by these DGs based on the loads in each time period. Furthermore, the controller resists against undesirable events and unmodeled system parameters or parameters that may have been overestimated or underestimated in their valuation and calculation.

In all the references mentioned, information on frequency control methods is provided, but the effect of microgrid structure and DG coefficient penetration on frequency control has not been studied in any of the

references. One of the microgrid design problems is regulating the penetration of DGs according to the microgrid frequency status. The microgrid frequency in the islanding mode is directly related to the DGs' penetration and type in the microgrid. It should be noted that the control method adopted for the microgrid also affects its frequency status.

Due to the low inertia of microgrids (because of the small scale of production and consumption), the microgrid control model parameters are changed. In this paper, to minimize the effect of changing control parameters on the microgrid frequency, a robust control method has been used. But this does not mean that changes in load and generation of microgrids do not affect the frequency variations. To find the effect of coefficient penetration on the frequency, different coefficients have been simulated, and the results have been investigated. Finally, using the proposed algorithms, the best coefficient penetration of these sources is obtained according to the microgrid frequency condition.

This paper uses a robust method for frequency control of a microgrid with a dual peak load profile. Load variation is one factor that affects the frequency stability, and a dual peak load profile has more load changes in a day and during the microgrid islanding mode. Simulations are carried out under different coefficient penetration of solar panels. In each case, the frequency deviation from the desired amount is calculated, and the results are compared. BESS available energy is a factor that can affect the frequency along with the solar coefficient penetration. However, it must be noted that the BESS available energy has economic constraints and can't increase as much as desired. An intelligent algorithm proposed, which determines the best value of the BESS and PV capacity according to frequency variation. This algorithm determines the percentage of power required (relative to the total power consumption of the micro-network) from the BESS by the IOE for the system operator. One of the items discussed in simulations is the amount of energy storage capacity in the microgrid and its effects on the maximum frequency deviations. Simulations test the effectiveness of the proposed method in the MATLAB/SIMULINK environment.

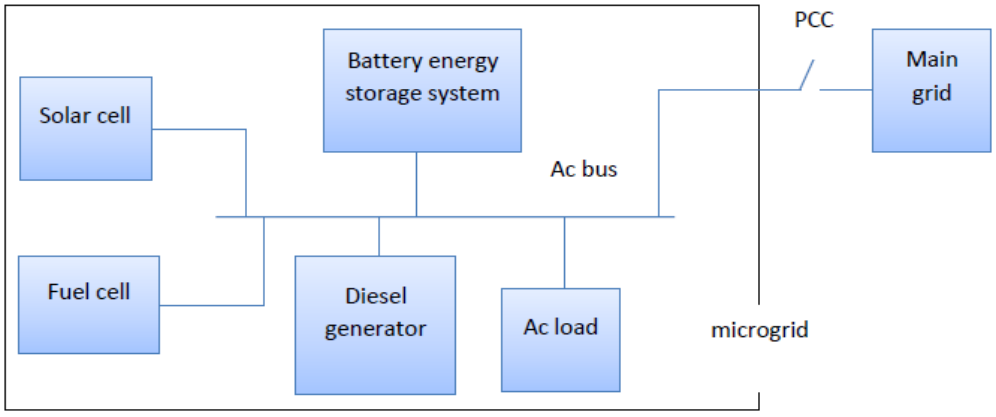

Fig. 1. Microgrid structure.

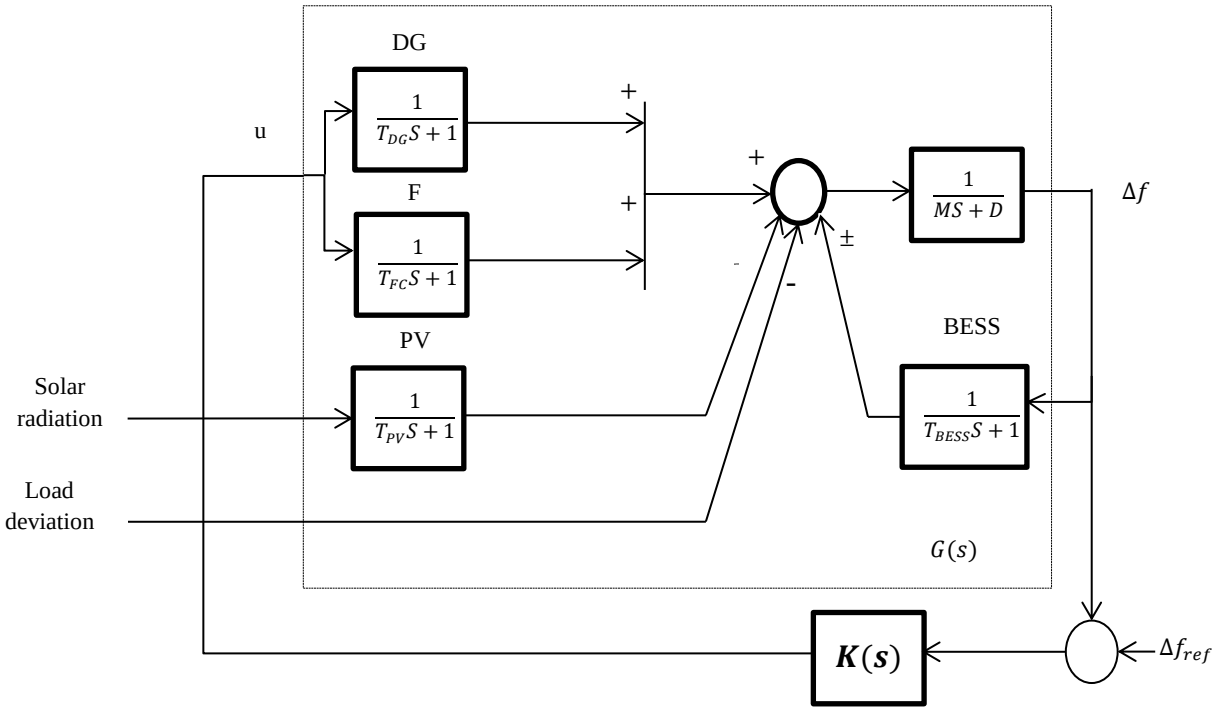

Fig. 2. Dynamical frequency model of a microgrid system [12].

2. MICROGRID STRUCTURE

In this study, a microgrid with the construction of Fig. 1 has been investigated. PCC is the point of microgrid connection with the main network. Opening the circuit breaker will change the microgrid mode to the islanding mode.

The dynamical frequency model of such a microgrid is shown in Fig. 2 [12]. Block K(s) demonstrates H_∞ frequency controller gain, which is discussed in the next section on its calculation. The frequency fluctuations of such a microgrid are controlled by adjusting the power generated by fuel cell and diesel generator units. Due to frequency fluctuations, the BESS may generate or store electrical power. The load fluctuations and the production of a solar unit are uncontrollable factors in this model. These values are considered as uncertainty parameters of the system. Using this model, the system conversion function can be obtained.

3. H_∞ FREQUENCY CONTROL METHOD

The $M-K$ standard block diagram of the H_∞ control method is as Fig. 3 [13].

The purpose of the H_∞ method is to find suitable $K(s)$, so that $z(s)$ will be minimized for arbitrary input $w(s)$. In other words, changes in the input do not affect adjustable

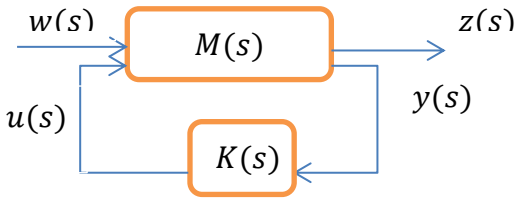

Fig. 3. The M-K standard display.

outputs. Matrices that can be obtained from the Fig. 3 are given in (1).

$$\begin{bmatrix} z \\ y \end{bmatrix} = M \begin{bmatrix} w \\ u \end{bmatrix} = \begin{bmatrix} M_{11}(s) & M_{12}(s) \\ M_{21}(s) & M_{22}(s) \end{bmatrix} \begin{bmatrix} w \\ u \end{bmatrix} \quad (1)$$

The conversion function from exogenous inputs to adjustable output (T_{zw}) is defined as Equation (2).

$$z(s) = T_{zw}(s)w(s) \quad (2)$$

In which T_{zw} according to Fig. 3 is as (3) [14]. T_{zw} is an important transformation function in the H_∞ method.

$$T_{zw} = M_{11} + M_{12}K(I - M_{22}K)^{-1}M_{21} \quad (3)$$

The state-space equations of a continuous linear time system are considered in Equation (4).

$$\begin{aligned} \dot{\boldsymbol{x}}(\boldsymbol{t}) &= \boldsymbol{A}\boldsymbol{x}(\boldsymbol{t}) + \boldsymbol{B_1}\boldsymbol{w}(\boldsymbol{t}) + \boldsymbol{B_2}\boldsymbol{u}(\boldsymbol{t}) \\ \boldsymbol{z}(\boldsymbol{t}) &= \boldsymbol{C_1}\boldsymbol{x}(\boldsymbol{t}) + \boldsymbol{D_{11}}\boldsymbol{w}(\boldsymbol{t}) + \boldsymbol{D_{12}}\boldsymbol{u}(\boldsymbol{t}) \\ y(t) &= C_2x(t) + D_{21}w(t) + D_{22}u(t) \end{aligned} \quad (4)$$

M is defined as Equation (5).

$$M = \begin{bmatrix} A & B_1 & B_2 \\ C_1 & D_{11} & D_{12} \\ C_2 & D_{21} & D_{22} \end{bmatrix} = \begin{bmatrix} M_{11}(s) & M_{12}(s) \\ M_{21}(s) & M_{22}(s) \end{bmatrix} \quad (5)$$

From the above matrix, it is found that the transfer functions M_{11}, M_{21}, M_{12} and M_{22} in (1) are as (6) [15].

$$\begin{aligned} M_{11} &= C_1(SI - A)^{-1}B_1 + D_{11} \\ M_{21} &= C_2(SI - A)^{-1}B_1 + D_{21} \\ M_{12} &= C_1(SI - A)^{-1}B_2 + D_{12} \\ M_{22} &= C_2(SI - A)^{-1}B_2 + D_{22} \end{aligned} \quad (6)$$

If state-space equations were given, M matrix and as a consequence T_{zw} can be calculated. The ideal value for T_{zw} is zero, but this value isn't possible. Therefore, a Threshold value is considered to have a possible manner. Thus, the objective of the H_∞ manner is to determine the implementation of H_∞ based frequency controller for an islanding microgrid [41]. In this method, the $K(s)$ must be found to minimize the infinity norm of T_{zw}.

H_∞ based frequency control is an appropriate method for microgrid frequency control due to a rapid reaction against consumption and generation active power variation.

Also, there are two advantages to H_∞ controller consisting of modeling fault and uncertainty response.

It must be noted that uncertainties will be so crucial in the islanding mode of the microgrid. Thus, the H_∞ method, which is a robust control method, can respond appropriately to these uncertainties. Fig. 4 represents a closed-loop block diagram for a microgrid, including structural uncertainty. This structure is achieved according to Fig. 2 and the topics discussed in this section for the mentioned microgrid. The parameters of the M-K standard mode for Fig. 2 are given in the appendix.

As shown in Fig. 4 $W_1(t)$ and $W_2(\mathrm{t})$ are solar variation and load deviation,

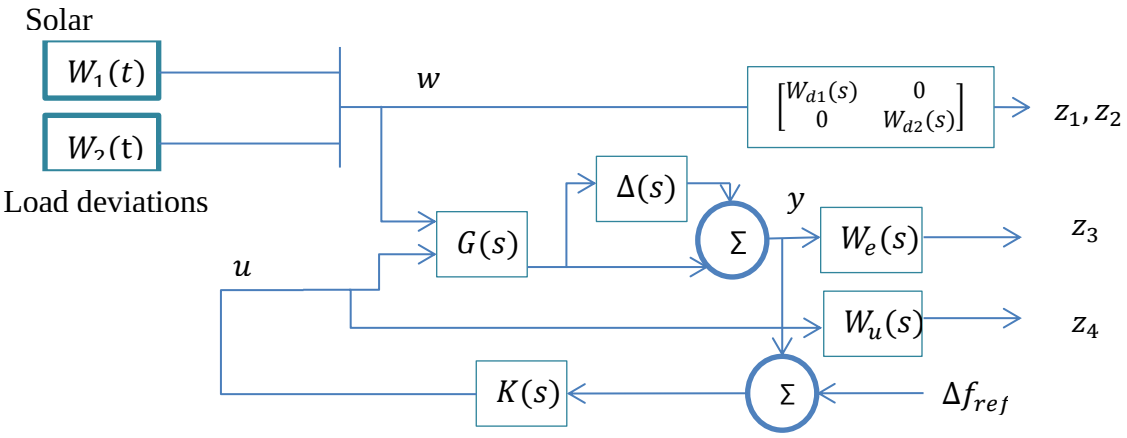

Fig. 4. Closed loop block diagram of a microgrid.

respectively, that microgrid frequency is changed by their time variations. z_1, z_2 are signals related to the power variation of uncontrolled inputs. z_3 is the signal that is related to system frequency changes and z_4 is the desired performance signal of controlled input.

$\Delta(s)$, $G(s)$ and $K(s)$ blocks indicate existence distortion conversion function, system conversion function and controller conversion function, respectively. $W_{d1}(s)$, $W_{d2}(s)$, $W_e(s)$ and $W_u(s)$ are weighting functions that provide output signals weight to achieving system optimal behaviors variation via system dynamic characteristics. These weighting functions are playing an important role in controller design. Due to the above weighting functions, a controller conversion function $K(s)$, is created that can be used to control the frequency of a microgrid with a low inertia coefficient.

However, it should be noted that different coefficient penetration of solar cells and BES (battery energy storage) available charge amount can affect microgrid frequency stability. An excessive increase in solar penetration cannot always improve the frequency profile and may be challenging when radiation is less. Furthermore, at times that the amount of solar radiation is insufficient and also the capacity of the BES charge isn't great, high penetration of solar units can cause inadequate supply in MG.

Considering these cases, one of the critical factors influencing the microgrid frequency in islanding condition is the amount of solar cell coefficient penetration. Hence, an algorithm is proposed to determine the best coefficient penetration for the solar cells and BES charge capacity to have minimum frequency deviation. This algorithm makes decision-based on frequency deviation from the acceptable value in each situation. The maximum frequency deviation of the grid, in each case, is given to the algorithm as input. Also, possible percentages of solar cell penetration and BES charge capacity are assigned to the algorithm as input.

In the Fig. 5 algorithm, the parameter 'Time' is the time intervals of a day that can be from 1 to 24. 'PV mode num' is the

different percentages of coefficient penetration of PV that can have different numbers based on structural constraints of the microgrid. 'BES mode num' is also different coefficient penetrations of BES.' calculated df' is the maximum frequency

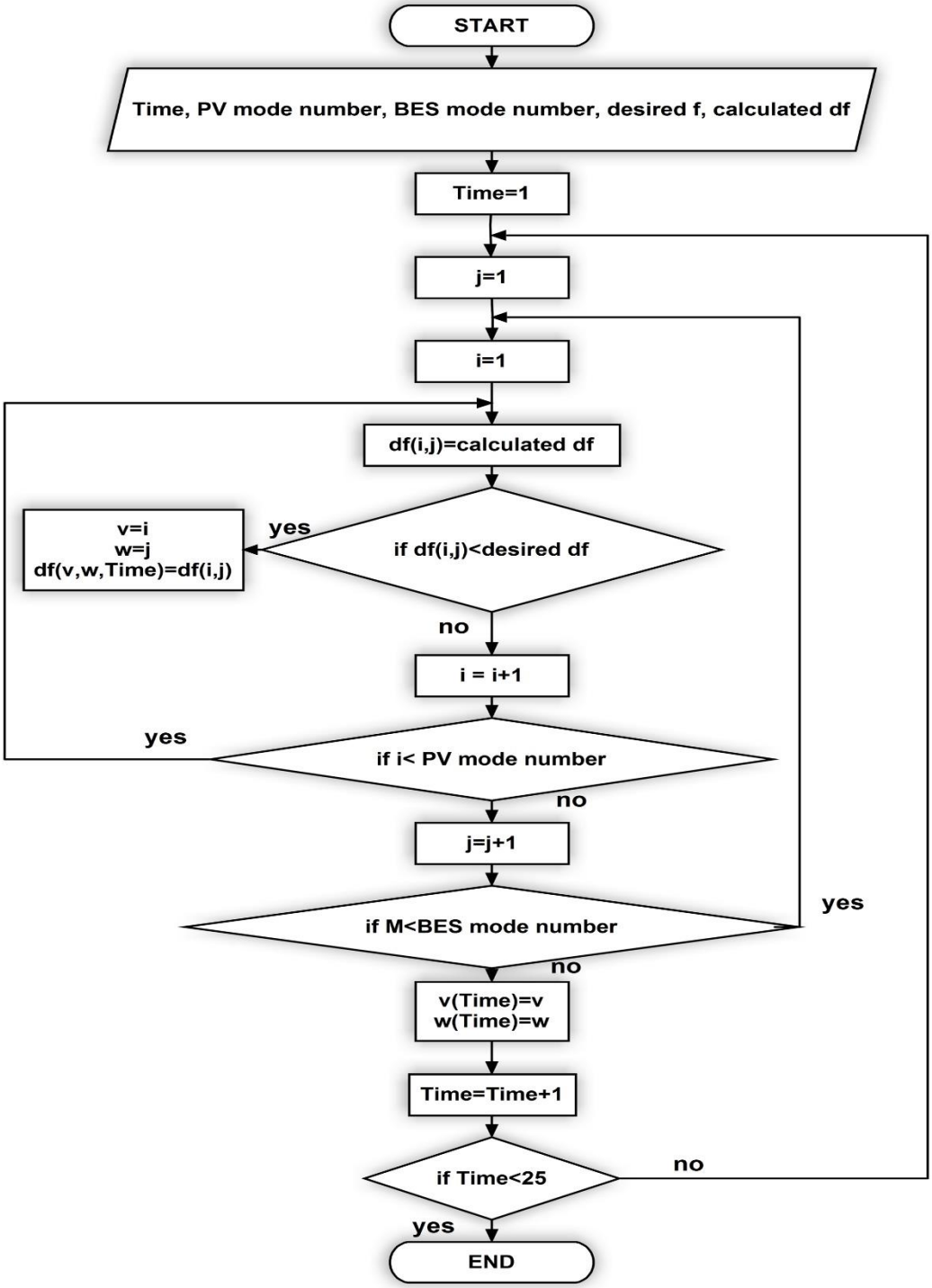

Fig. 5. Algorithm for calculating minimum frequency deviation for each time period.

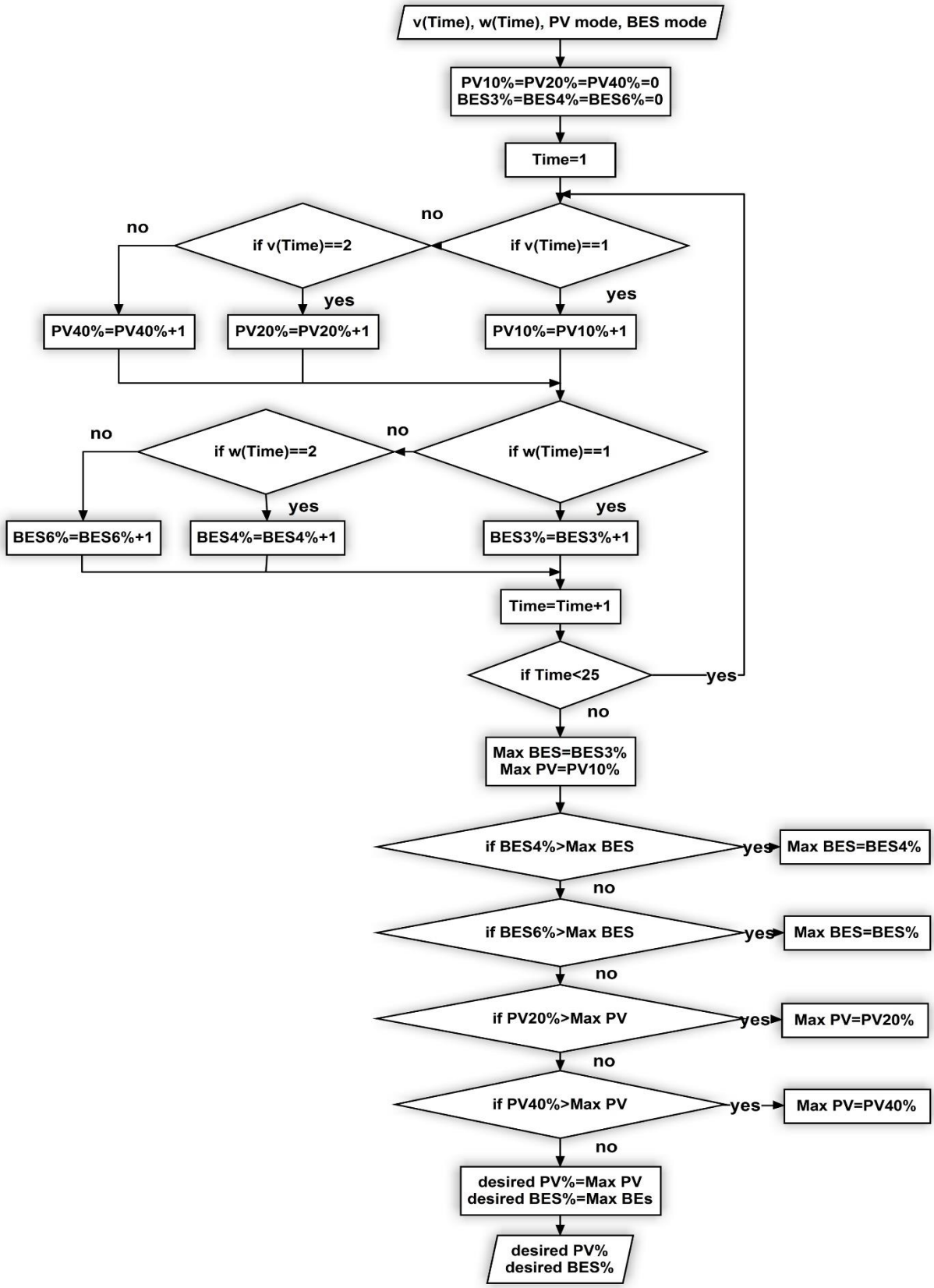

Fig. 6. Optimal mode computing algorithm.

deviation caused by a specific error that occurs at any time obtained from the simulation results for a specific amount of PV BES coefficient penetration. Also, in this algorithm, *i*, *P* are indices related to PV and *j*, *V*, are the indices related to the BES states.

Fig. 5 shows the algorithm that calculates the minimum frequency deviation for each time period of a day. The output information of this algorithm is used in the second algorithm, and finally, the second algorithm determines the best mode.

In Fig. 5, $v(Time)$ and $w(Time)$ indicate modes in which the lowest frequency deviation occurs for each time period. As can be seen, outputs of the second algorithm are acceptable solar penetration and battery capacity, which is obtained according to the microgrid structure, load and production of other units' conditions.

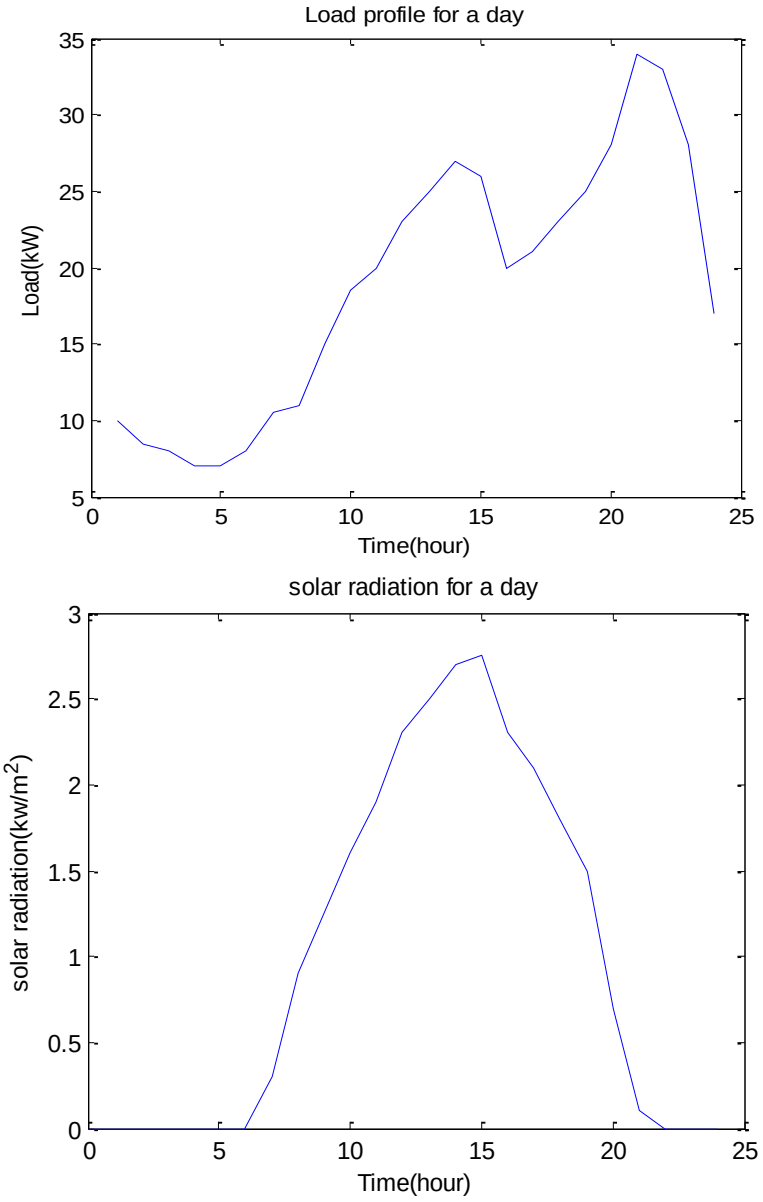

Fig. 7. Load profile ($W_1(t)$) and solar radiation ($W_2(t)$) for the simulation.

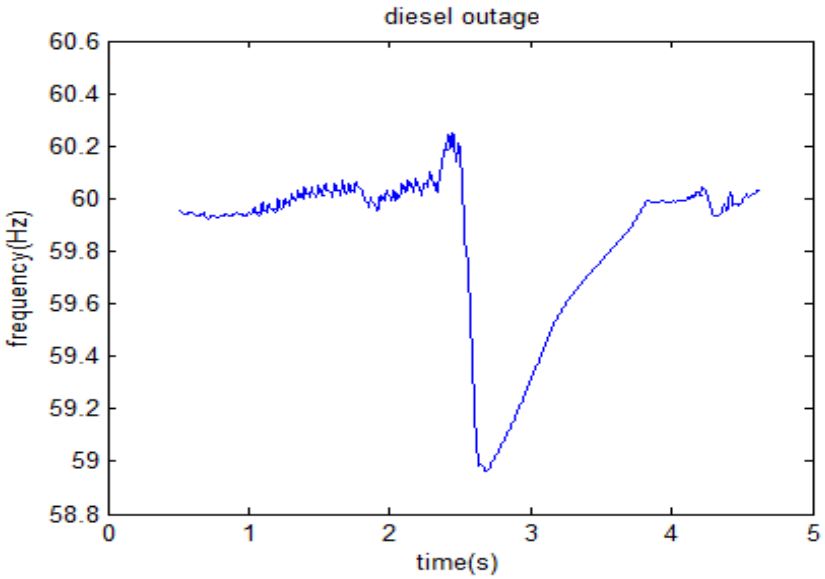

Fig. 8. Load frequency profile in the absence of diesel generator.

4. RESULTS AND DISCUSSION

H_∞ frequency control results for the microgrid presented in the previous section have been studied in the following scenarios. Undetermined factors are system M and D parameters, that M is the system inertia, and D is microgrid damping coefficient, which is applied to the system as feedforward $\Delta(s)$. In order to obtain $K(s)$ the range of changes to these parameters is considered to be 50%. The load profile and solar radiation for this simulation are as Fig. 7.

One of the most critical factors affecting the controller design is the determination of weighting functions. There is no mathematical method or a particular algorithm for obtaining these weighting functions. The trial and error method and observation of these functions' effects on the output are used to get them. Weighting functions that use for the case study network of this article are as Equation (7).

$$W_e(s) = \frac{.007s^3 + s^2 + 10s + 40}{2s^3 + 10s^2 + 150s + 6}$$
$$W_u(s) = \frac{6(.2s + 1)}{s^2 + 500s + 1000} \quad (7)$$
$$W_d(s) = \begin{bmatrix} .15 & 0 \\ 0 & .15 \end{bmatrix}$$

In this study, the values of $M(pu/s)$ and $D(pu/Hz)$ are 0.2 and 0.015, respectively. Also, the time constants T_{DG}, $T_{FC}(s)$, $T_{PV}(s)$ and $T_{PEV}(s)$ are 2, 3, 1.8 and 0.5, respectively.

4.1. First Scenario: Diesel Generator Outage

In this scenario, after the network goes to islanding mode, the diesel generator unit is departed from the network. Fig. 8 represents the simulation results of microgrid load frequency in the absence of a diesel generator.

In this simulation, the amount of solar radiation is 3000w/m^2. As can be seen from the figures, in this case, frequency deviation

from the permissible limit can damage the sensitive equipment. Diesel outage in this situation, due to considering that diesel generator is one of the sources that its production is affected by frequency control gain, has a severe impact on the system's inertia. As a result, system inertia variation is more than 50% of the consideration amount and therefore designed $K(s)$ cannot properly control the microgrid frequency.

4.2. Second Scenario: Frequency Control Due to Solar Unit Uncertainty

In this scenario, the performance of H_∞ frequency controller, due to the solar unit generation changes, is investigated. These uncertainties are related to the different generations of solar cells at different times of the day. In this article, a microgrid with a dual peak load profile has been investigated. The first peak is considered to be 3-5 pm and the

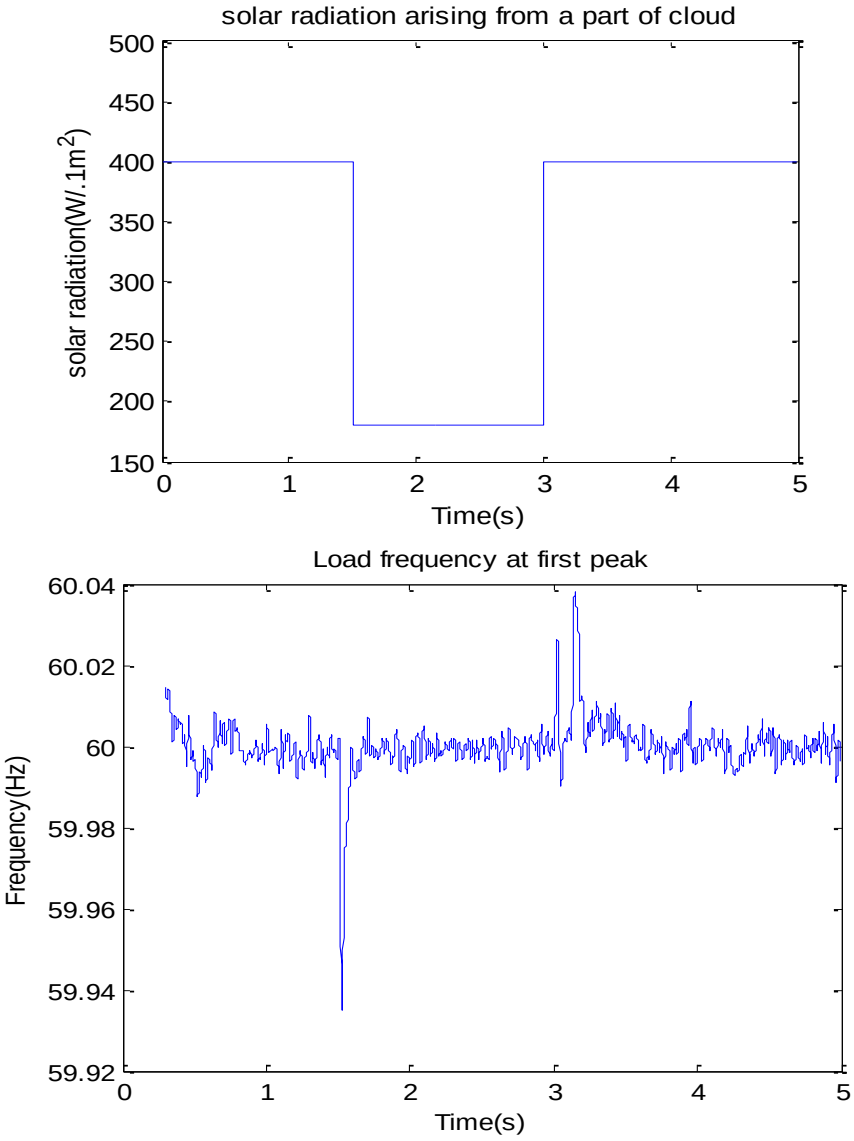

Fig. 9. Load frequency (first peak time).

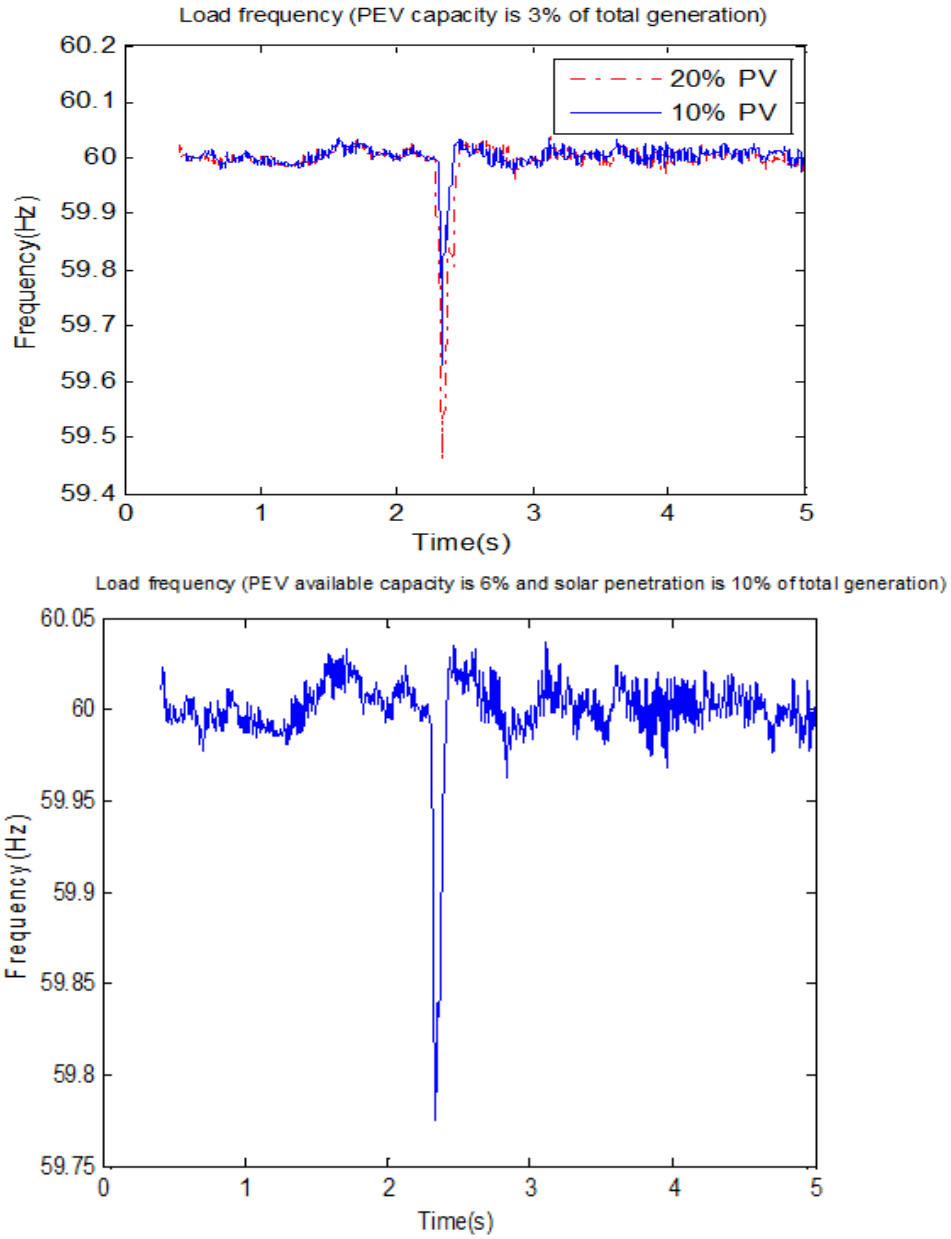

Fig. 10. Load frequency (second peak time).

second one from 7 to 11 pm in a day. Fig. 9 shows the microgrid load frequency based on solar radiation changes making by using a piece of cloud against the solar panel at the first peak time.

In the second peak, since there is no sunlight, the frequency profile with BES available capacity changes is shown in fig. 10. In this case, load changes are applied to the system as uncertainty.

In [42] similar simulations are performed on a sample microgrid, and two robust methods control the frequency of a microgrid. Also, in this paper, using the H_∞ frequency control method, the frequency of the microgrid is controlled in the presence of uncertainties. But the operating conditions

and load profile of microgrids in islanding mode can significantly affect frequency fluctuations. At the second peak time, by increasing the percentage of solar unit generation compared with total production (because there is no solar generation in this interval), frequency stability meets more problems. For this reason, it can't be said that increasing the percentage of solar generation will undoubtedly improve frequency control. So determining the rate of solar cells and BES available capacity is very important in controlling the system's frequency. The algorithm presented in the previous section specifies the best values of these generators.

4.3. Third Scenario: Frequency Deviation in Different Coefficient Penetration of Solar Panels and Different Quantities of BES Capacity

Solar cells and BES systems in a microgrid can provide different amounts of network generation capacity. Different coefficient penetration of these generators directly affects the microgrid frequency. The coefficient penetration for solar cells is considered 10, 20 and 40 percent of total generation. Simulations are carried out at different periods depending on the different quantities of the available BES charge and solar cell, and the results of the frequency variations are given in figures 11 to 13. These results are obtained for a microgrid with a dual peak load model in islanding mode. The maximum acceptable frequency fluctuation in the grid is $\pm 1\%$. In these simulations, the maximum deviation of the base value frequency is considered the result.

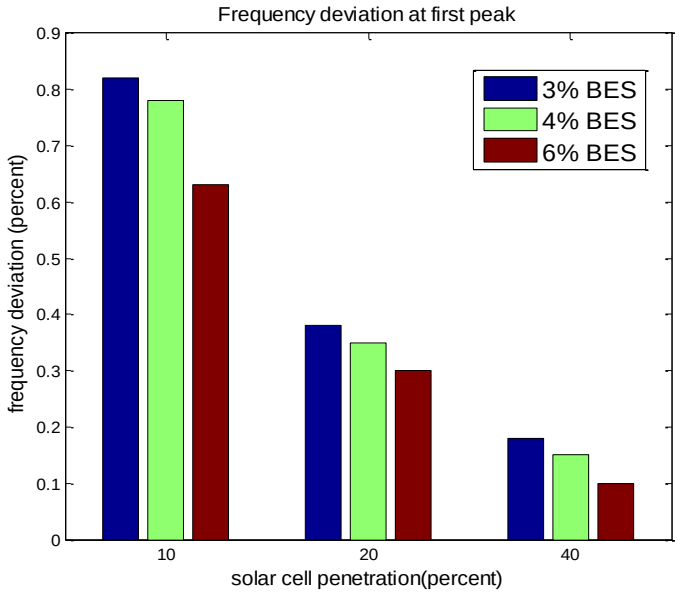

Fig. 11. Frequency deviation of an islanded microgrid with different coefficient penetration of solar cell at the first peak.

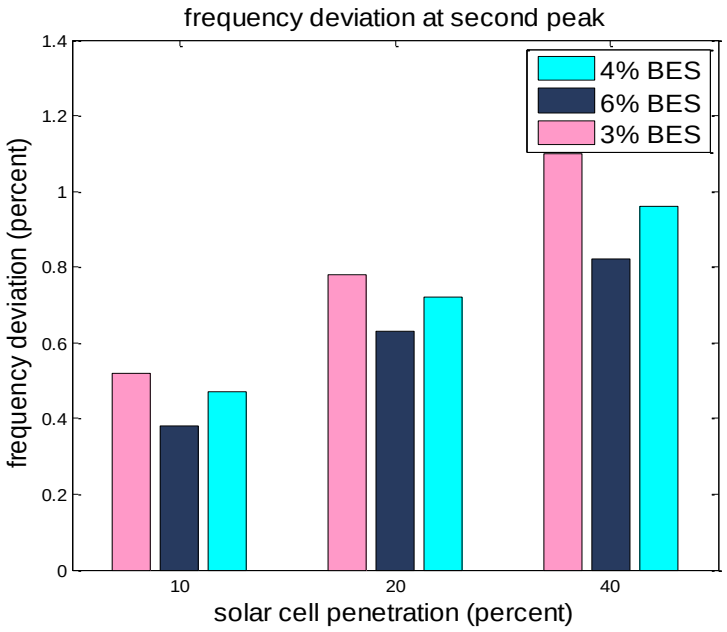

Fig. 12. Frequency deviation of an islanded microgrid with different coefficient penetration of solar cell at the second peak.

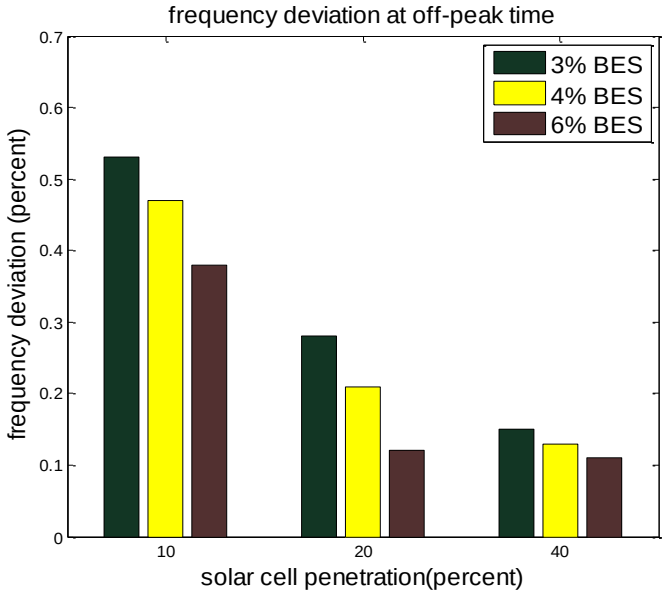

Fig. 13. Frequency deviation of an islanded microgrid with different coefficient penetration of solar cell at the off-peak time.

For all simulations that lead to the results presented in these figures, the uncertainty and disorder considered for the microgrid are the same for all modes. In Fig. 11, since the amount of solar radiation is maximum, uncertainties do not affect the frequency when the amount of solar cell penetration is high. Increasing BES capacity has a positive

impact on the frequency profile in all cases. Fig. 12 represents the frequency deviation of an islanded microgrid at the second peak period. There is no sunlight in this period, and as a result, the generation of the solar unit is zero.

The high percentage of solar cells, which prevents the frequency in the first peak time, causes the frequency to drop out of the allowed range. BES capacity has a positive effect on frequency, but the increasing size is subject to financial constraints. Fig. 13 shows the frequency variation in the off-peak night period.

ACKNOWLEDGMENT

This paper proposes a robust method for frequency control of a microgrid with a dual peak load profile. To achieve this goal, a robust H_∞ technique is implemented to control the frequency of an islanded microgrid in the presence of uncertainties. The H_∞ based controller is designed to reduce the uncertainties of the solar power fluctuation and load disturbances and dynamic perturbation. Simulations are carried out under different coefficient penetration of solar panels. In each case, the frequency deviation from the desired amount is calculated, and the results are compared. If the PI control was used in this simulation, due to the fact that the system inertia is reduced in the islanding mode and uncertainties affect microgrid parameters, the frequency fluctuations and the duration of the frequency stabilization increase compared to the H_∞ method. The H_∞ method, as its name implies, is a robust method that resists parameter changes. According to the results, the best penetration for a solar cell is 20% for a microgrid with such a configuration (for this case study). Also, the best penetration for BES capacity is 6% in this study. Ultimately, an algorithm is proposed to precisely determine the best coefficient penetration of the solar cell and the BES capacity with respect to different network structures.

APPENDIX

$$x = \begin{bmatrix} \Delta P_{DG} \\ \Delta P_{FC} \\ \Delta P_{SC} \\ \Delta P_{PEV} \\ \Delta f \end{bmatrix} \qquad w = \begin{bmatrix} \Delta P_{solar} \\ \Delta P_{Load} \end{bmatrix}$$

$$y = \Delta f$$

$$A = \begin{bmatrix} -1/T_{DG} & 0 & 0 & 0 & 0 \\ 0 & -1/T_{FC} & 0 & 0 & 0 \\ 0 & 0 & -1/T_{SC} & 0 & 0 \\ 0 & 0 & 0 & -1/T_{PEV} & 1/T_{PEV} \\ 1/M & 1/M & 1/M & -1/M & -D/M \end{bmatrix}$$

$$B_1 = \begin{bmatrix} 0 & 0 \\ 0 & 0 \\ 1/T_{SC} & 0 \\ 0 & 0 \\ 0 & 1/M \end{bmatrix} \quad B_2 = \begin{bmatrix} 1/T_{DG} \\ 1/T_{FC} \\ 0 \\ 0 \\ 0 \end{bmatrix}$$

$$C_2 = [0 \quad 0 \quad 0 \quad 0 \quad 1]$$

$$C_1 = D_{11} = D_{12} = D_{21} = D_{22} = 0$$

NOMENCLATURE

MG	microgrid
WT	wind turbine
PV	photovoltaic
BESS	battery energy storage system
MT	micro-turbine
FC	fuel cell
DG	distributed generation
IOE	Internet of energy
PCC	point of common coupling

T_{DG} time constant of diesel generator
T_{FC} time constant of fuel cell
T_{PV} time constant of photovoltaic system
T_{BESS} time constant of battery energy storage system
D system damping factor
M system inertia constant
$K(s)$ controller gain
$G(s)$ nominal model of the system
$w(s)$ exogenous inputs that can't be controlled
$u(s)$ controlled inputs
$z(s)$ adjustable outputs
$y(s)$ measured outputs

REFERENCES

[1] N. Natziargyriou, H. Asano, R. Iravani and C. Marnay, Microgrids, IEEE power and energy magazine, vol. 5, No. 4, pp. 78-94, 2007.

[2] X. Tang, X. Hu, N. Li, W. Deng and G. Zhang, A novel frequency and voltage control method for islanded microgrid based on multienergy storages, IEEE Trans. Smart Grid, vol. 7, No. 1, pp. 410-419, 2016.

[3] Z. Zhao, P. Yang, J. M. Guerrero, Z. Xu and T. C. Green, Multiple-time-scales hierarchical frequency stability control strategy of medium-voltage isolated microgrid, IEEE Trans. Power Electron., vol. 31, No. 8, pp. 5974 - 5991, 2016.

[4] J. M. Guerrero, M. Chandorkar, T. L. Lee and P. C. Loh, Advanced control architectures for intelligent microgrids-part 1: decentralized and hierarchical control, IEEE Trans. Ind. Electron., vol. 60, No. 4, pp. 1254-1262, 2013.

[5] M. Wooldridge, "Intelligent Agents, " Cambridge, MIT Press, 1999, pp. 3-51.

[6] C. Y. Chang and W. Zhang, Distributed control of inverter-based lossy microgrids for power sharing and frequency regulation under voltage constraints, Automatica, vol. 66, pp. 85-95, 2016.

[7] M. S. Sadabadi, A. Karimi and H. Karimi, Fixed-order decentralized/distributed control of islanded inverter-interfaced microgrids, Control Eng. Practice, vol. 45, pp. 174-193, 2015

[8] M. M. Rezaei and J. Soltani, Robust control of an islanded multi-bus microgrid based on input–output feedback linearisation and sliding mode control, IET Generation, Transmission & Distribution, vol. 9, No. 15, pp. 2447 - 2454, 2015.

[9] Q. L. Lam, A. I. Bratcu and D. Riu, Robustness analysis of primary frequency H∞ control in stand-alone microgrids with storage units, IFAC-PapersOnLine, vol. 49, No. 27, pp. 123-128, 2016.

[10] K. F. Krommydas and A. T. Alexandridis, Modular control design and stability analysis of isolated PV-source/battery-storage distributed generation systems, IEEE Journal on Emerging and Selected Topics in Circuits and Systems, vol. 5, No. 3, pp. 372 - 382, 2015.

[11] Y. Sun, Y. Wang, Z. Wei, G. Sun and X. Wu, Robust H∞ Load Frequency Control of Multi-area Power System

With Time Delay: a Sliding Mode Control Approach, IEEE/CAA Journal of Automatica Sinica, vol. 5, No. 2, pp. 610-617, 2018.

[12] H. Bevrani, F. Habibi, P. Babahajyani, M. Watanabe and a. Y. Mitani, Intelligent frequency control in an AC microgrid: Online PSO-based, IEEE Trans. Smart Grid, vol. 3, No. 4, pp. 1935-1944, 2012.

[13] N.Chuang, Robust H∞ Load-Frequency Control in Interconnected Power Systems, IET Control Theory & Applications, vol. 10, No. 1, pp. 67-75, 2016.

[14] S. Ghorbani and S. Ghazi-Maghrebi, A Novel Detection Method Based on Enhanced Diagonal Secant Updating Frequency Domain Fourth-Order Cumulant Scheme for DSSS Signals, Signal Processing and Renewable Energy, vol. 4, No. 3, pp. 41-55, 2020.

[15] S. Kumari and G. Shankar, Maiden application of cascade tilt-integral-derivative controller in load frequency control of deregulated power system, *Int Trans Electr Energ Syst*. 2020; 30:e12257.

[16] E. Weitenberg, Y. Jiang, C. Zhao, E. Mallada, C. De Persis and F. Dörfler, "Robust Decentralized Secondary Frequency Control in Power Systems: Merits and Tradeoffs," in IEEE Transactions on Automatic Control, vol. 64, no. 10, pp. 3967-3982, Oct. 2019, doi: 10.1109/TAC.2018.2884650.

[17] T. Kerdphol, F. S. Rahman, M. Watanabe and Y. Mitani, "Robust Virtual Inertia Control of a Low Inertia Microgrid Considering Frequency Measurement Effects," in IEEE Access, vol. 7, pp. 57550-57560, 2019, doi: 10.1109/ACCESS.2019.2913042.

[18] S. A. Hosseini, M. Toulabi, A. S. Dobakhshari, A. Ashouri-Zadeh and A. M. Ranjbar, "Delay Compensation of Demand Response and Adaptive Disturbance Rejection Applied to Power System Frequency Control," in IEEE Transactions on Power Systems, vol. 35, no. 3, pp. 2037-2046, May 2020, doi: 10.1109/ TPWRS .2019. 2957125.

[19] H. Kim, M. Zhu and J. Lian, "Distributed Robust Adaptive Frequency Control of Power Systems with Dynamic Loads," in IEEE Transactions on Automatic Control, vol. 65, no. 11, pp. 4887-4894, Nov. 2020, doi: 10.1109/TAC.2019.2962356.

[20] Y. Arya, "Effect of electric vehicles on load frequency control in interconnected thermal and hydrothermal power systems utilising CF-FOIDF controller," in IET Generation, Transmission & Distribution, vol. 14, no. 14, pp. 2666-2675, 17 7 2020, doi: 10.1049/iet-gtd.2019.1217.

[21] M. H. Syed, E. Guillo-Sansano, A. Mehrizi-Sani and G. M. Burt, "Load Frequency Control in Variable Inertia Systems," in IEEE Transactions on Power Systems, vol. 35, no. 6, pp. 4904-4907, Nov. 2020, doi: 10.1109/TPWRS.2020.3014778.

[22] Aali, SR, Besmi, MR, Kazemi, MH. Adaptive filtering with robust

controller for improvement of inertial response of wind turbine. *Int Trans Electr Energ Syst*. 2019;e12089.

[23] H. Tao, W. Paszke, H. Yang and K. Gałkowski, Finite frequency range robust iterative learning control of linear discrete system with multiple time-delays, Journal of the Franklin Institute, vol. 356, No. 5, pp. 2690 – 2708, 2019.

[24] H. Jing, R. Wang, C. Li and J. Bao, Robust finite-frequency H∞ control of full-car active suspension, Journal of Sound and Vibration, Vol. 441, pp. 221-239, 2019.

[25] A. H. Tayebi, R. Sharifi, A. H. Salemi and F. Faghihi, Presentation of an Algorithm for Identification of the Most Vulnerable Bus in Electric Smart Grid Through Cyber-Attack Based on State Estimation, Advanced Defence Sci. & Tech. vol. 11, pp. 391-401,2020.

[26] V. Repecho, D. Biel, J. M. Olm, E. Fossas,Robust sliding mode control of a DC/DC Boost converter with switching frequency regulation, Journal of the Franklin Institute, vol. 355, No. 13, pp. 5367-5383, 2018.

[27] R. Huang, Y. Xu, W. Yao, L. Hoegner and U. Stilla, Robust global registration of point clouds by closed-form solution in the frequency domain, ISPRS Journal of Photogrammetry and Remote Sensing, vol. 171, pp. 310-329, 2021.

[28] A. Ahmadi and M. Aldeen, Robust overlapping load frequency output feedback control of multi-area interconnected power systems, International Journal of Electrical Power & Energy Systems, vol. 89, pp. 156-172, 2017.

[29] L. Xiong, H. Li and J. Wang, LMI based robust load frequency control for time delayed power system via delay margin estimation, International Journal of Electrical Power & Energy Systems, vol 100, pp. 91-103, 2018.

[30] C. Jiang, J. Zhou, P. Shi, W. Huang and D. Gan, Ultra-low frequency oscillation analysis and robust fixed order control design, International Journal of Electrical Power & Energy Systems, vol 104, pp. 269-278, 2019.

[31] N. M. Nor, W. Steeneveld, M. C. M. Mourits ang H. Hogeveen, The optimal number of heifer calves to be reared as dairy replacements, Journal of Dairy Science, vol. 98, No. 2, pp. 861-871, 2015.

[32] G. Wang, C. Chen and S. Yu, Robust non-fragile finite-frequency H∞ static output-feedback control for active suspension systems, Mechanical Systems and Signal Processing, Vol. 91, pp. 41-56, 2017.

[33] A. Krishna, J. Schiffer and J. Raisch, Distributed secondary frequency control in microgrids: Robustness and steady-state performance in the presence of clock drifts, European Journal of Control, vol. 51, pp. 135-145, 2020.

[34] Y. Cui, L. Xu, M. Fei and Y. Shen,Observer based robust integral sliding mode load frequency control for wind power systems, Control Engineering Practice, vol. 65, pp. 1-10, 2017.

[35] M. Godfrey and K. D. Singh, Measuring robust functional connectivity from resting-state MEG using amplitude and entropy correlation across frequency bands and temporal scales, NeuroImage, vol. 226, 2021.

[36] A. Pradhan, N. Jiang, V. Chester and U. Kuruganti, Linear regression with frequency division technique for robust simultaneous and proportional myoelectric control during medium and high contraction-level variation, Biomedical Signal Processing and Control, vol. 61, 2020.

[37] L Bhukya, A. Annamraju and N. Srikanth, Robust frequency control in a wind-diesel autonomous microgrid: A novel two-level control approach, Renewable Energy Focus, vol. 36, pp. 21-30, 2021.

[38] A. H. Tayebi, r. Sharifi, A. H. Salemi and F. Faghihi, Presentation of an H_∞ based frequency control for islanding provisional microgrid consisting of hybrid AC/DC microgrid. *Int Trans Electr Energ Syst*. 2020;e12715.

[39] T. Kerdphol, F. S. Rahman, Y. Mitani, M. Watanabe and S. Küfeoğlu, Robust virtual inertia control of an islanded microgrid considering high penetration of renewable energy, IEEE Access, vol. 6, pp. 625 - 636, 2017.

[40] A. Fathi, Q. Shafiee and H. Bevrani, Robust frequency control of microgrids using an extended virtual synchronous generator, IEEE Trans. Power Sys., vol. 33, No. 6, pp. 6289 - 6297, 2018.

[41] S. Ebrahimi, A. Moghassemi and J. Olamaei, PV Inverters and Modulation Strategies: A Review and A Proposed Control Strategy for Frequency and Voltage Regulation, Signal Processing and Renewable Energy, vol. 4, No. 1, pp. 1-21, 2020.

[42] H. Bevrani, M. R. Feizi and S. Ataee, Robust frequency control in an islanded microgrid: H∞ and μ-synthesis approaches, IEEE Trans. Smart Grid, vol. 7, No. 2, pp. 706 - 717, 2016